Dodecahedral space topology as an explanation for weak wide-angle temperature correlations in the cosmic microwave background

Jean-Pierre Luminet[1], **Jeffrey R. Weeks**[2], **Alain Riazuelo**[3], **Roland Lehoucq**[1,3] **& Jean-Philippe Uzan**[4]

[1]*Observatoire de Paris, 92195 Meudon Cedex, France*
[2]*15 Farmer Street, Canton, New York 13617-1120, USA*
[3]*CEA/Saclay, 91191 Gif-sur-Yvette Cedex, France*
[4]*Laboratoire de Physique Théorique, Université Paris XI, 91405 Orsay Cedex, France*

The current 'standard model' of cosmology posits an infinite flat universe forever expanding under the pressure of dark energy. First-year data from the Wilkinson Microwave Anisotropy Probe (WMAP) confirm this model to spectacular precision on all but the largest scales[1,2]. Temperature correlations across the microwave sky match expectations on angular scales narrower than 60° but, contrary to predictions, vanish on scales wider than 60°. Several explanations have been proposed[3,4]. One natural approach questions the underlying geometry of space—namely, its curvature[5] and topology[6]. In an infinite flat space, waves from the Big Bang would fill the universe on all length scales. The observed lack of temperature correlations on scales beyond 60° means that the broadest waves are missing, perhaps because space itself is not big enough to support them. Here we present a simple geometrical model of a finite space—the Poincaré dodecahedral space—which accounts for WMAP's observations with no fine-tuning required. The predicted density is $\Omega_0 \approx 1.013 > 1$, and the model also predicts temperature correlations in matching circles on the sky[7].

Temperature fluctuations on the microwave sky may be expressed as a sum of spherical harmonics, just as music and other sounds may be expressed as a sum of ordinary harmonics. A musical note is the sum of a fundamental, a second harmonic, a third harmonic, and so on. The relative strengths of the harmonics—the note's spectrum—determines the tone quality, distinguishing, say, a sustained middle C played on a flute from the same note played on a clarinet. Analogously, the temperature map on the microwave sky is the sum of spherical harmonics. The relative strengths of the harmonics—the power spectrum—is a signature of the physics and geometry of the Universe. Indeed, the power spectrum is the primary tool researchers use to test their models' predictions against observed reality.

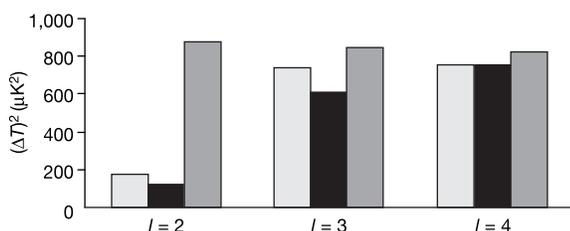The infinite universe model gets into trouble at the low end of the

Figure 1 Comparison of the WMAP power spectrum to that of Poincaré dodecahedral space and an infinite flat universe. At the low end of the power spectrum, WMAP's results (black bars) match the Poincaré dodecahedral space (light grey) better than they match the expectations for an infinite flat universe (dark grey). Computed for $\Omega_m = 0.28$ and $\Omega_\Lambda = 0.734$ with Poincaré space data normalized to the $l = 4$ term.

power spectrum (Fig. 1). The lowest harmonic—the dipole, with wavenumber $l = 1$—is unobservable because the Doppler effect of the Solar System's motion through space creates a dipole 100 times stronger, swamping out the underlying cosmological dipole. The first observable harmonic is the quadrupole, with wavenumber $l = 2$. WMAP found a quadrupole only about one-seventh as strong as would be expected in an infinite flat space. The probability that this could happen by mere chance has been estimated at about 0.2% (ref. 2). The octopole term, with wavenumber $l = 3$, is also weak at 72% of the expected value, but not nearly so dramatic or significant as the quadrupole. For large values of l, ranging up to $l = 900$ and corresponding to small-scale temperature fluctuations, the spectrum tracks the infinite universe predictions exceedingly well.

Cosmologists thus face the challenge of finding a model that accounts for the weak quadrupole while maintaining the success of the infinite flat universe model on small scales (high l). The weak wide-angle temperature correlations discussed in the introductory paragraph correspond directly to the weak quadrupole.

Microwave background temperature fluctuations arise primarily (but not exclusively) from density fluctuations in the early Universe, because photons travelling from denser regions do a little extra work against gravity and therefore arrive cooler, while photons from less dense regions do less work against gravity and arrive warmer. The density fluctuations across space split into a sum of three-dimensional harmonics—in effect, the vibrational overtones of space itself—just as temperature fluctuations on the sky split into a sum of two-dimensional spherical harmonics and a musical note splits into a sum of one-dimensional harmonics. The low quadrupole implies a cut-off on the wavelengths of the three-dimensional harmonics. Such a cut-off presents an awkward problem in infinite flat space, because it defines a preferred length scale in an otherwise scale-invariant space. A more natural explanation invokes a finite universe, where the size of space itself imposes a cut-off on the wavelengths (Fig. 2). Just as the vibrations of a bell cannot be larger than the bell itself, the density fluctuations in space cannot be larger than space itself. Whereas most potential spatial topologies fail to fit the WMAP results, the Poincaré dodecahedral space fits them very well.

The Poincaré dodecahedral space is a dodecahedral block of space with opposite faces abstractly glued together, so objects passing out of the dodecahedron across any face return from the opposite face. Light travels across the faces in the same way, so if we sit inside the
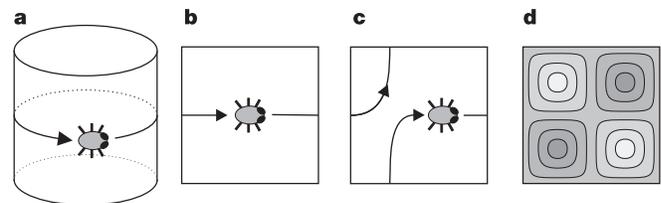

Figure 2 Wavelengths of density fluctuations are limited by the size of a finite 'wraparound' universe. **a**, A two-dimensional creature living on the surface of a cylinder travels due east, eventually going all the way around the cylinder and returning to her starting point. **b**, If we cut the cylinder open and flatten it into a square, the creature's path goes out of the square's right side and returns from the left side. **c**, A flat torus is like a cylinder, only now the top and bottom sides connect as well as the left and right. **d**, Waves in a torus universe may have wavelengths no longer than the width of the square itself. To construct a multiconnected three-dimensional space, start with a solid polyhedron (for example, a cube) and identify its faces in pairs, so that any object leaving the polyhedron through one face returns from the matching face. Such a multiconnected space supports standing waves whose exact shape depends on both the geometry of the polyhedron and how the faces are identified. Nevertheless, the same principle applies, that the wavelength cannot exceed the size of the polyhedron itself. In particular, the inhabitants of such a space will observe a cut-off in the wavelengths of density fluctuations.

 593

dodecahedron and look outward across a face, our line of sight re-enters the dodecahedron from the opposite face. We have the illusion of looking into an adjacent copy of the dodecahedron. If we take the original dodecahedral block of space not as a euclidean dodecahedron (with edge angles ~117°) but as a spherical dodeca-hedron (with edge angles exactly 120°), then adjacent images of the dodecahedron fit together snugly to tile the hypersphere (Fig. 3b), analogously to the way adjacent images of spherical pentagons (with perfect 120° angles) fit snugly to tile an ordinary sphere (Fig. 3a).

The power spectrum of the Poincaré dodecahedral space depends strongly on the assumed mass-energy density parameter Ω_0 (Fig. 4). The octopole term ($l = 3$) matches WMAP's octopole best when $1.010 < \Omega_0 < 1.014$. Encouragingly, in the subinterval $1.012 < \Omega_0 < 1.014$ the quadrupole ($l = 2$) also matches the WMAP value. More encouragingly still, this subinterval agrees well with observations, falling comfortably within WMAP's best-fit range of $\Omega_0 = 1.02 \pm 0.02$ (ref. 1).

The excellent agreement with WMAP's results is all the more striking because the Poincaré dodecahedral space offers no free parameters in its construction. The Poincaré space is rigid, meaning that geometrical considerations require a completely regular dode-cahedron. By contrast, a 3-torus, which is nominally made by gluing opposite faces of a cube but may be freely deformed to any parallelepiped, has six degrees of freedom in its geometrical con-struction. Furthermore, the Poincaré space is globally homo-geneous, meaning that its geometry—and therefore its power spectrum—looks statistically the same to all observers within it. By contrast, a typical finite space looks different to observers sitting at different locations.

Confirmation of a positively curved universe ($\Omega_0 > 1$) would require revisions to current theories of inflation, but it is not certain how severe those changes would be. Some researchers argue that positive curvature would not disrupt the overall mechanism and effects of inflation, but only limit the factor by which space expands during the inflationary epoch to about a factor of ten[8]. Others claim that such models require fine-tuning and are less natural than the infinite flat space model[9].

Having accounted for the weak observed quadrupole, the Poin-caré dodecahedral space will face two more experimental tests in the next few years. (1) The Cornish–Spergel–Starkman circles-in-the-sky method[7] predicts temperature correlations along matching circles in small multiconnected spaces such as this one. When $\Omega_0 \approx 1.013$ the horizon radius is about 0.38 in units of the curvature radius, while the dodecahedron's inradius and outradius are 0.31 and 0.39, respectively, in the same units. In this case the horizon sphere self-intersects in six pairs of circles of angular radius about 35°, making the dodecahedral space a good candidate for circle detection if technical problems (galactic foreground removal, inte-grated Sachs–Wolfe effect, Doppler effect of plasma motion) can be overcome. Indeed, the Poincaré dodecahedral space makes circle searching easier than in the general case, because the six pairs of matching circles must a priori lie in a symmetrical pattern like the faces of a dodecahedron, thus allowing the searcher to slightly relax the noise tolerances without increasing the danger of a false positive. (2) The Poincaré dodecahedral space predicts $\Omega_0 \approx 1.013 > 1$. The upcoming Planck Surveyor data (or possibly even the existing WMAP data in conjunction with other data sets) should determine Ω_0 to within 1%. Finding $\Omega_0 < 1.01$ would refute the Poincaré space as a cosmological model, while $\Omega_0 > 1.01$ would provide strong evidence in its favour.
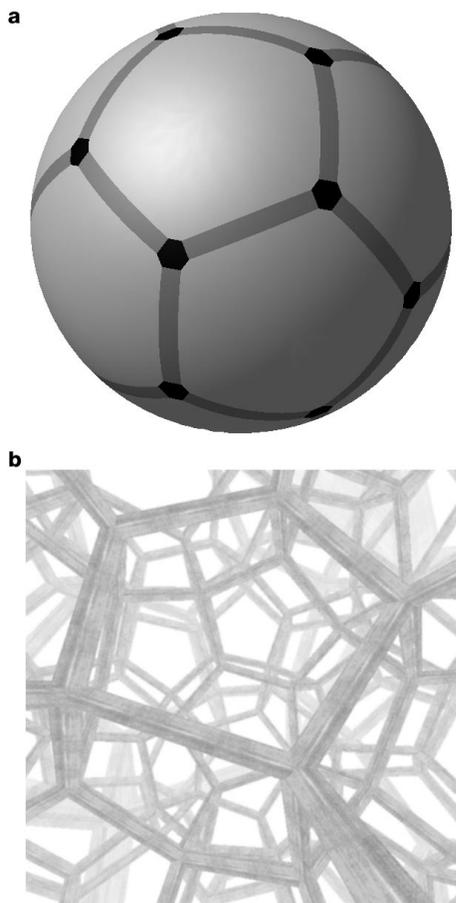

Figure 3 Spherical pentagons and dodecahedra fit snugly, unlike their euclidean counterparts. **a**, 12 spherical pentagons tile the surface of an ordinary sphere. They fit together snugly because their corner angles are exactly 120°. Note that each spherical pentagon is just a pentagonal piece of a sphere. **b**, 120 spherical dodecahedra tile the surface of a hypersphere. A hypersphere is the three-dimensional surface of a four-dimensional ball. Note that each spherical dodecahedron is just a dodecahedral piece of a hypersphere. The spherical dodecahedra fit together snugly because their edge angles are exactly 120°. In the construction of the Poincaré dodecahedral space, the dodecahedron's 30 edges come together in ten groups of three edges each, forcing the dihedral angles to be 120° and requiring a spherical dodecahedron rather than a euclidean one. Software for visualizing spherical dodecahedra and the Poincaré dodecahedral space is available at 〈http://www.geometrygames.org/CurvedSpaces〉.
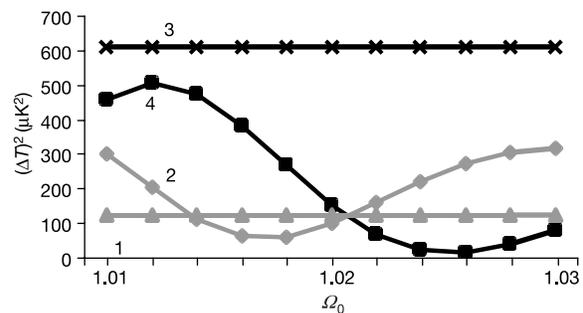

Figure 4 Values of the mass-energy density parameter Ω_0 for which the Poincaré dodecahedral space agrees with WMAP's results. The Poincaré dodecahedral space quadrupole (trace 2) and octopole (trace 4) fit the WMAP quadrupole (trace 1) and octopole (trace 3) when $1.012 < \Omega_0 < 1.014$. Larger values of Ω_0 predict an unrealistically weak octopole. To obtain these predicted values, we first computed the eigenmodes of the Poincaré dodecahedral space using the 'ghost method' of ref. 10 with two of the matrix generators computed in Appendix B of ref. 11, and then applied the method of ref. 12, using $\Omega_m = 0.28$ and $\Omega_\Lambda = \Omega_0 - 0.28$, to obtain a power spectrum and to simulate sky maps. Numerical limitations restricted our set of three-dimensional eigenmodes to wavenumbers $k < 30$, which in turn restricted the reliable portion of the power spectrum to $l = 2, 3, 4$. We set the overall normalization factor to match the WMAP data at $l = 4$ and then examined the predictions for $l = 2, 3$.

Since antiquity, humans have wondered whether our Universe is finite or infinite. Now, after more than two millennia of speculation, observational data might finally settle this ancient question. ☐

1. Bennett, C. L. *et al.* First year Wilkinson Microwave Anisotropy Probe (WMAP 1) observations: Preliminary maps and basic results. *Astrophys. J. Suppl.* **148**, 1–27 (2003).
2. Spergel, D. N. *et al.* First year Wilkinson Microwave Anisotropy Probe (WMAP 1) observations: Determination of cosmological parameters. *Astrophys. J. Suppl.* **148**, 175–194 (2003).
3. Contaldi, C. R., Peloso, M., Kofman, L. & Linde, A. Suppressing the lower multipoles in the CMB anisotropies. *J. Cosmol. Astropart. Phys.* **07**, 002 (2003).
4. Cline, J. M., Crotty, P. & Lesgourgues, J. Does the small CMB quadrupole moment suggest new physics? *J. Cosmol. Astropart. Phys.* (in the press); preprint at ⟨http://arXiv.org/astro-ph/0304558⟩ (2003).
5. Efstathiou, G. Is the low CMB quadrupole a signature of spatial curvature? *Mon. Not. R. Astron. Soc.* **343**, L95–L98 (2003).
6. Tegmark, M., de Oliveira-Costa, A. & Hamilton, A. A high resolution foreground cleaned CMB map from WMAP. *Phys. Rev. D* (in the press); preprint at ⟨http://arXiv.org/astro-ph/0302496⟩ (2003).
7. Cornish, N., Spergel, D. & Starkman, G. Circles in the sky: Finding topology with the microwave background radiation. *Class. Quant. Grav.* **15**, 2657–2670 (1998).
8. Uzan, J.-P., Kirchner, U. & Ellis, G. F. R. WMAP data and the curvature of space. *Mon. Not. R. Astron. Soc.* (in the press).
9. Linde, A. Can we have inflation with $\Omega > 1$? *J. Cosmol. Astropart. Phys.* **05**, 002 (2003).
10. Lehoucq, R., Weeks, J., Uzan, J.-P., Gausmann, E. & Luminet, J.-P. Eigenmodes of 3-dimensional spherical spaces and their application to cosmology. *Class. Quant. Grav.* **19**, 4683–4708 (2002).
11. Gausmann, E., Lehoucq, R., Luminet, J.-P., Uzan, J.-P. & Weeks, J. Topological lensing in spherical spaces. *Class. Quant. Grav.* **18**, 5155–5186 (2001).
12. Riazuelo, A., Uzan, J.-P., Lehoucq, R. & Weeks, J. Simulating cosmic microwave background maps in multi-connected spaces. *Phys. Rev. D* (in the press); preprint at ⟨http://arXiv.org/astro-ph/0212223⟩ (2002).

Correspondence and requests for materials should be addressed to J.R.W. (weeks@northnet.org).

· ·

Fermi-liquid breakdown in the paramagnetic phase of a pure metal

N. Doiron-Leyraud[1], **I. R. Walker**[1], **L. Taillefer**[2], **M. J. Steiner**[1], **S. R. Julian**[1] & **G. G. Lonzarich**[1]

[1]*Cavendish Laboratory, University of Cambridge, Cambridge CB3 0HE, UK*
[2]*Département de Physique, Université de Sherbrooke, Québec J1K 2R1, Canada*

· ·

Fermi-liquid theory[1] (the standard model of metals) has been challenged by the discovery of anomalous properties in an increasingly large number of metals. The anomalies often occur near a quantum critical point—a continuous phase transition in the limit of absolute zero, typically between magnetically ordered and paramagnetic phases. Although not understood in detail, unusual behaviour in the vicinity of such quantum critical points was anticipated nearly three decades ago by theories going beyond the standard model[2–5]. Here we report electrical resistivity measurements of the 3d metal MnSi, indicating an unexpected breakdown of the Fermi-liquid model—not in a narrow crossover region close to a quantum critical point[6,7] where it is normally expected to fail, but over a wide region of the phase diagram near a first-order magnetic transition. In this regime, corrections to the Fermi-liquid model are expected to be small. The range in pressure, temperature and applied magnetic field over which we observe an anomalous temperature dependence of the electrical resistivity in MnSi is not consistent with the crossover behaviour widely seen in quantum critical systems[8,9,31]. This may suggest the emergence of a well defined but enigmatic quantum phase of matter.

In the investigation of anomalous metallic properties, often referred to as non-Fermi-liquid phenomena, complications of various types may arise that can lead to ambiguous interpretations. These can be related, for example, to band structure anomalies, to magneto-crystalline anisotropies, to the effective dimensionality or to disorder effects. In other materials, the emergence of superconductivity may make it difficult to probe the fundamental nature of the normal state of the underlying electronic system. In order to conclusively assess and clarify our ideas about non-Fermi-liquid phenomena in metals, it is essential to study materials that fulfil the desirable criteria of purity, simplicity and convenience. The itinerant-electron ferromagnet MnSi appears to be one such example[10]. Under ambient conditions of pressure and applied magnetic field, MnSi orders ferromagnetically with a small average moment of up to 0.4 μ_B per Mn atom (where μ_B is the Bohr magneton) and a Curie temperature T_C of 29.5 K (ref. 11). At low temperatures, it exhibits properties consistent with the formation of a weakly spin-polarized Fermi liquid dominated by moderately renormalized 3d bands. With its full three-dimensional cubic crystal structure, the electronic and magnetic properties of MnSi are essentially isotropic, except for the effects of a well-understood long-wavelength helical twist of the ferromagnetic order characteristic of crystalline structures lacking inversion symmetry—such as the B20 lattice of MnSi (ref. 12).

The possibility of producing ultra-pure single crystals of MnSi with a disorder mean free path in excess of 5,000 Å (as confirmed by
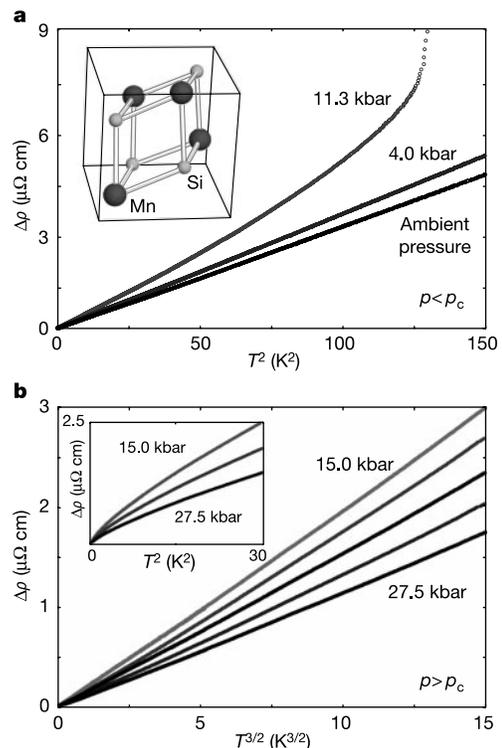

Figure 1 Dependence on temperature of the electrical resistivity of MnSi. The temperature-dependent part $\Delta\rho$ of the resistivity above the residual resistivity $\rho_0 = 0.17\,\mu\Omega\,\text{cm}$ is plotted for different conditions of pressure. **a**, $\Delta\rho$ on a quadratic temperature scale up to about 12 K and for pressures below the critical pressure, that is, in the ferromagnetic phase. As the Curie temperature is suppressed with pressure, the quadratic regime is observed only below about 6 K at 11.3 kbar. Inset, the cubic unit cell of the B20 lattice of MnSi. **b**, $\Delta\rho$ on a scale of $T^{3/2}$ up to about 6 K and for pressures above the critical pressure, that is, in the paramagnetic phase. From top to bottom, the pressures are 15.0, 18.1, 19.6, 25.3 and 27.5 kbar. The clear departure from a quadratic behaviour is shown in the inset for 15.0, 19.6 and 27.5 kbar.

 595